ADVANCED ENERGY & SUSTAINABILITY RESEARCH
Open Access
www.advenergysustres.com

Inhibition of Corrosion in Alkaline Silicon–Air Batteries with Polyethylene Glycol

*Richard Schalinski, Paula Mörstedt, Stefan L. Schweizer, and Ralf. B. Wehrspohn**

Silicon–air batteries (SABs) are attracting significant attention for their potential as high-energy-density electrochemical storage devices. One of the main limitations for the commercial use of alkaline SABs is the high corrosion, which results in a low conversion efficiency. Herein, the aim is to examine the influence of polyethylene glycol (PEG) on the conversion efficiency of SABs, shedding light on key factors affecting their performance. SABs using KOH as electrolyte at two concentrations, 0.5 and 2.0 mol L^{-1}, are investigated. The results show that replacing part of the water in the alkaline electrolyte with PEG changes the etching behavior from anisotropic to polishing and increases the specific energy density by 53% and 123% in 0.5 and 2 mol L^{-1} KOH electrolytes, respectively.

1. Introduction

Metal–air batteries gained attention in recent years due to their high theoretical energy densities.[1] They consist of a negative electrode composed of metal and a positive gas diffusion electrode. The oxygen in the air is used as the active material for the positive electrode, making it a lightweight battery with a large capacity.[2] Besides metals, semiconductors like Ge and Si were also investigated in this system.[3–5] Silicon–air batteries (SABs) use silicon as the negative electrode. The full-cell discharging and side reactions of the SAB in alkaline electrolytes are described in Equation (1–4)

$$\text{Anode (oxidation)}\ \mathrm{Si} + 4\mathrm{OH^-} \rightarrow \mathrm{Si(OH)_4} + 4\mathrm{e^-} \quad (1)$$

$$\text{Cathode (reduction)}\ \mathrm{O_2} + 2\mathrm{H_2O} + 4\mathrm{e^-} \rightarrow 4\,\mathrm{OH^-} \quad (2)$$

$$\text{Global reaction (red} - \text{ox)}\ \mathrm{Si} + \mathrm{O_2} + 2\mathrm{H_2O} \rightarrow \mathrm{Si(OH)_4} \quad (3)$$

Competing parasitic corrosion reaction:

$$\mathrm{Si} + 2\mathrm{OH^-} + 2\mathrm{H_2O} \rightarrow \mathrm{SiO_2(OH)_2^{2-}} + 2\mathrm{H_2} \quad (4)$$

While rechargeability has been demonstrated for silicon-redox batteries with an electrolyte comprising fluorohydrogenates and bromide and a halide cathode at room temperature and for a SAB with a solid electrolyte at 800 °C, the stability window of aqueous electrolytes like the KOH used here prohibits recharge.[6,7] Corrosion is a major concern in SABs, particularly in the context of large electrode surfaces. High levels of corrosion can lead to significant structural degradation, which in turn can prohibit the use of high currents over large areas.[8] One strategy for reducing corrosion is to lower the concentration of the potassium hydroxide (KOH) used as electrolyte, as lower concentrations have resulted in lower levels of corrosion.[4,9] However, an extreme reduction of the KOH concentration can result in discharge durations that are too short for practical use.[9] Therefore, an important goal is to enable the use of SABs by reducing corrosion while keeping a long lifetime. The main focus in the research on alkaline SABs has been modifying the silicon electrode to increase the discharge duration.[4,8,10–12] A refilling system that pumped electrolyte solution in intervals into an SAB and enabled complete consumption of a 3 mm-thick electrode showed the role of the electrolyte for the discharge duration before passivation of the Si-electrode.[5] The underlying mechanism for prolonged discharge is to keep a low silicate concentration in the bulk electrolyte, which directly influences the diffusion of reaction products away from the silicon surface.[9] If a threshold concentration of silicates is exceeded, the reaction products of the corrosion cannot be transported off the surface and a passivating oxide layer grows on the silicon.[9] Various additives were investigated for corrosion inhibition in other metal–air battery systems.[13–17] Organic molecules like polyethylene glycol (PEG), benzotriazol, and Tween were used in Zn–air batteries with alkaline electrolytes.[18–22] Although corrosion has also been identified as a relevant problem of SABs in alkaline electrolytes, to the best of the authors' knowledge, there are no reports on modifications of the alkaline electrolyte for SABs.[23] Polyethylene oxides, with molecular weights above 20 kg mol^{-1}, were also used for alkaline gel polymer electrolytes as a solid structure with a conduction mechanism similar to liquid electrolytes for metal–air batteries.[24,25] In contrast, in this work, we investigate how liquid PEG with a molecular weight of 400 g mol^{-1} as a solvent with KOH impacts the corrosion and

R. Schalinski, P. Mörstedt, S. L. Schweizer, R. B. Wehrspohn
Department of Physics
Martin-Luther University
Heinrich-Damerow-Str. 4, 06120 Halle, Germany
E-mail: ralf.wehrspohn@physik.uni-halle.de

R. B. Wehrspohn
Korea Institute of Energy Technology (KENTECH)
21 Kentech-gil, Naju 58330, South Korea

The ORCID identification number(s) for the author(s) of this article can be found under https://doi.org/10.1002/aesr.202300138.

DOI: 10.1002/aesr.202300138

discharge behavior of full SABs. PEG as a polymer has been extensively studied and is nontoxic and biocompatible.[26] It exhibits low volatility, reducing the risk of hazardous emissions during battery operation, being a nonhazardous substitution to water. Glembocki et al. report that H_2O etching is prevalent at low KOH concentrations, whereas the H_2O/OH^- etching becomes more dominant above 2 mol L^{-1} KOH.[27] The etching process is heavily influenced by water, as alcohol/KOH solutions without water do not allow etching. However, etching can occur even in pure H_2O when the pure silicon surface is mechanically exposed.[28] The electron lone pair of oxygen within the water molecule facilitates the cleavage of the Si–Si backbond and prompts the H-proton to form a Si–H bond in subsurface silicon.[29–31] The performance of SABs with water-free ionic liquids improves with the addition of water.[32] In alkaline electrolytes, OH is consumed during the discharge of the SABs to produce $SiO_2(OH)_2^{2-}$, which necessitates replenishment through the cathodic reaction of water with oxygen. The approach of this work is to decrease the water content by replacing it with a neutral solvent (PEG) while keeping the OH- concentration constant. Whenever the etch rate is restricted by water at low KOH concentrations,[27] this decrease in water is believed to decrease undesired chemical reactions. Since water plays a crucial role in the dissolving process, it is believed that there is a certain threshold beyond which the discharge properties will deteriorate.

2. Results and Discussion

We investigated the effect of PEG-containing KOH electrolyte on the unwanted chemical and electrochemical corrosion of the silicon in the SAB during discharge. The variation of etch rate in n-Si in response to potential has been established in previous studies.[30,33,34] Consequently, we expect that the loss of silicon to side reactions during the discharge process in SABs with PEG in the electrolyte will also deviate from values obtained in corrosion experiments conducted at open circuit potential (OCP).[23] The corrosion of silicon in alkaline solutions has been examined in previous studies using electrochemical polarization measurements and step and weight loss measurements.[23,27,34–36] These studies uncovered a chemical and an electrochemical component in the corrosion process, with the electrochemical component being two orders of magnitude smaller than the chemical one. As corrosion reduction was high, we focused specifically on the chemical component here by measuring the total weight lost.

2.1. Electrochemical Performance in Low pH Electrolyte

We investigated the effect of different concentrations of PEG with 0.5 mol L^{-1} KOH electrolyte on the electrochemical performance of SABs. The focus is on the inhibition of parasitic corrosion. One measure for this is the conversion efficiency as the ratio of electrochemically consumed silicon to the total amount of consumed silicon during the experiment.[5] The substitution of water by PEG in the SABs caused a conversion efficiency increase from 9% in pure 0.5 mol L^{-1} KOH electrolyte to 15% in the SAB with 1.5 mol L^{-1} PEG (**Figure 1**a). Additionally, the specific energy exhibited an upward trend, increasing from 250 up to 384 Wh kg_{Si}^{-1} despite a slight decrease in the average voltage, which can be seen in the discharge profiles in the supplementary information (Figure S1, Supporting Information). Increasing PEG concentration affected the solutions' viscosity and therefore their conductivity, particularly above 0.1 mol L^{-1} (Figure 1b). The enhanced viscosity can hinder the diffusion of the reaction products from the silicon surface into the bulk electrolyte, which could result in silicon electrode passivation.[9] Therefore, we examined the discharge time until the voltage dropped below 0.4 V for different PEG concentrations to determine an effect on the passivation (Figure S2, Supporting Information). Despite a reduction in conductivity, from 110 mS cm^{-1} in pure 0.5 mol L^{-1} KOH electrolyte to 30 mS cm^{-1} with 1 mol L^{-1} PEG, the discharge time increased from 50 h without PEG to 58 h with the addition of PEG (Figure 1c). However, this difference is within the measurement error and therefore PEG has no influence up to this concentration. Nevertheless, a further increase of the PEG concentration reduced the duration of discharge before passivation, so that the silicon electrode was no longer dischargeable at a PEG content of 2 mol L^{-1}.

To investigate the effects of the PEG content on the air electrode, we performed discharge tests in the full cell setup with an additional reversible hydrogen electrode as the reference. The potential of the air electrode in 0.5 mol L^{-1} KOH electrolyte gradually declined during discharge until the voltage of the cell dropped (Figure 1d). Conversely, the presence of 1 mol L^{-1} PEG led to a slow decline in the potential of the air electrode until it reached the value of the pure KOH electrolyte at the end of discharge. Moreover, the silicon electrode's potential increased with the addition of 1 mol L^{-1} PEG, resulting in a 0.07 V shift toward positive potentials in comparison to the pure 0.5 mol L^{-1} KOH electrolyte. Higher overpotentials may account for the altered potential of the silicon electrode with PEG as a result of its lower conductivity. The fact that the OCV is actually higher with the addition of PEG suggests a kinetic effect (Figure S1, Supporting Information).

The characteristic sudden voltage drop at the end of discharge can be attributed to the passivation of the silicon electrode.[9,37] Although the experiments show average voltages as low as 0.7 V at higher PEG content, the reduction in corrosion outweighs the voltage, leading to an increase in specific energy. Even with an OCV of around 1.4 V, the experimentally determined voltage is much lower than the theoretical value. However, various values have been reported in the literature regarding the theoretical voltage of the silicon–air system. It is generally accepted that a 4 electron reaction occurs. In an electrolyte comprising an ionic liquid at ambient temperature, Cohn et al. reported a hypothetical potential of 2.16 V and determined an OCV of ≈1.5 V.[38] In an alkaline electrolyte, Zhong et al. proposed a theoretical potential of 2.09 V with experimental OCVs reaching up to 1.4 V.[4]. Weinrich et al. have reported the alkaline electrolyte potentials for $Si/Si(OH)_4$) and Si/SiO_2 to be 2.09 and 2.21 V, respectively.[35] Inoishi et al. reported theoretical potentials of 0.958 V for Si/SiO and 1.821 V for Si/SiO_2, which varied greatly from the others.[7] They determined the mixed potential of their high-temperature oxygen shuttling solid electrolyte system by measuring the open-circuit voltage of 1.34 V. Establishing the theoretical voltage is difficult because of the unknown variables during discharge for both the chemical and electrochemical components of the etching process. It is possible that there is a mixed

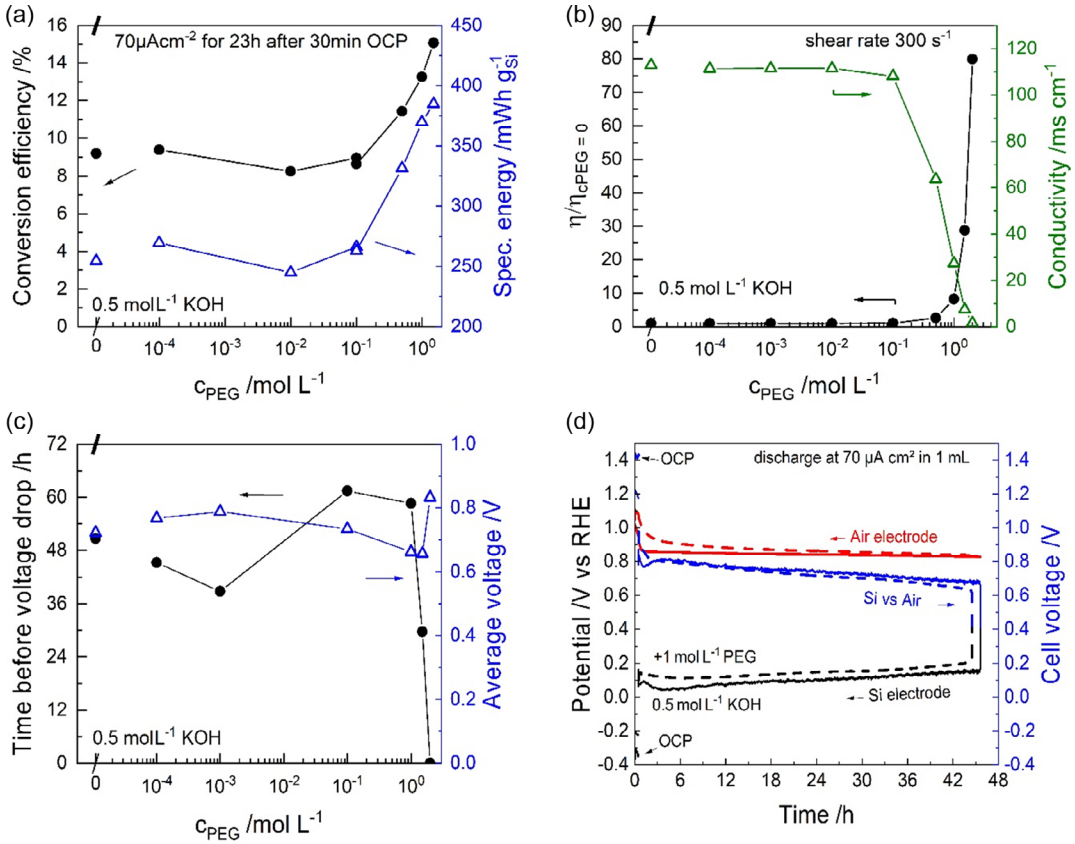

Figure 1. Discharge of SABs at 70 μA cm^{-2} in 0.5 mol L^{-1} KOH solution with varying PEG 400 content a) the conversion efficiency and specific energy for 23 h after 30 min at OCP, b) the change in viscosity and conductivity due to replacement of water by PEG, c) the time before the passivation of the Si-electrode and the average voltage of the same cell, and d) the potentials of the Si- and air-electrode of a full SAB with respect to RHE reference electrode until passivation for pure 0.5 mol L^{-1} KOH (—) and with 1 mol L^{-1} PEG content (— · —).

potential, owing to shared intermediates in both reactions, as observed by Philipsen et al.[29] This is supported by the notably lower open-circuit voltage of no more than 1.5 V in published experimental data, including this one, and operating voltages below 1.2 V.

To investigate the corrosion behavior at different discharge rates, discharge tests were conducted in pure 0.5 mol L^{-1} KOH and with 1.5 mol L^{-1} PEG across a current density range of 10–70 μA cm^{-2}. **Figure 2**a,b shows the discharge profiles and as expected the overpotential increases with increasing current density. Up till 30 μA cm^{-2}, the voltage is higher for the additional 1.5 mol L^{-1} PEG in the first 24 h. Above this current, the voltage reduces faster with PEG. The efficiency of the SABs consistently increases with the discharge current (Figure 2d). The highest achievable current without immediate passivation of the silicon electrode was found to be 70 μA cm^{-2} for the solution containing 0.5 mol L^{-1} KOH, which did not change with the addition of PEG. For the 0.5 mol L^{-1} KOH solution, the conversion efficiency increased approximately fivefold, from 1.8% at 10 μA cm^{-2} to 9.1% at 70 μA cm^{-2}. Similarly, the inclusion of 1.5 mol L^{-1} PEG into the KOH solution increased the conversion efficiency almost fivefold, from 3.1% at 10 μA cm^{-2} to 15% at 70 μA cm^{-2}. Up to 30 μA cm^{-2}, the addition of PEG does not affect the conversion efficiency trajectory. However, above this value, we observe a steady increase in efficiency with the addition of PEG, whereas the KOH electrolyte alone reaches a plateau around 9%. We measured the parasitic corrosion in pure 0.5 mol L^{-1} KOH solution at OCV which is around 0.18 μm h^{-1} but is subject to large variations in repeating measurements (Figure 2c). Although in the same range, our values were slightly lower than the 0.33 μm h^{-1} reported by Durmus et al. with highly As-doped (100) silicon wafers as electrodes.[23] The difference in results could be attributed to our use of phosphorus-doped silicon in the experiments and possible variations in the limited electrolyte volume during the 24 h etching duration. While we used P-doped Si with a resistivity of 1–10 Ω cm ($n < 10^{16}$), Durmus et al. utilized highly As-doped Si with a resistivity of 0.001–0.007 Ω cm ($n > 10^{19}$) which could increase the electrochemical etch rate. The corrosion rate without any current flow in the presence of 1.5 mol L^{-1} PEG is 0.25 μm h^{-1}, which is within the error margin of the pure 0.5 mol L^{-1} KOH. The mainly chemical side reactions increase with discharge current, potentially due to shared intermediates of the chemical and electrochemical etching process.[23,31] The rise is notably more pronounced for the pure KOH electrolyte in comparison to the supplemented PEG, indicating a substantial edge of the PEG at higher currents.

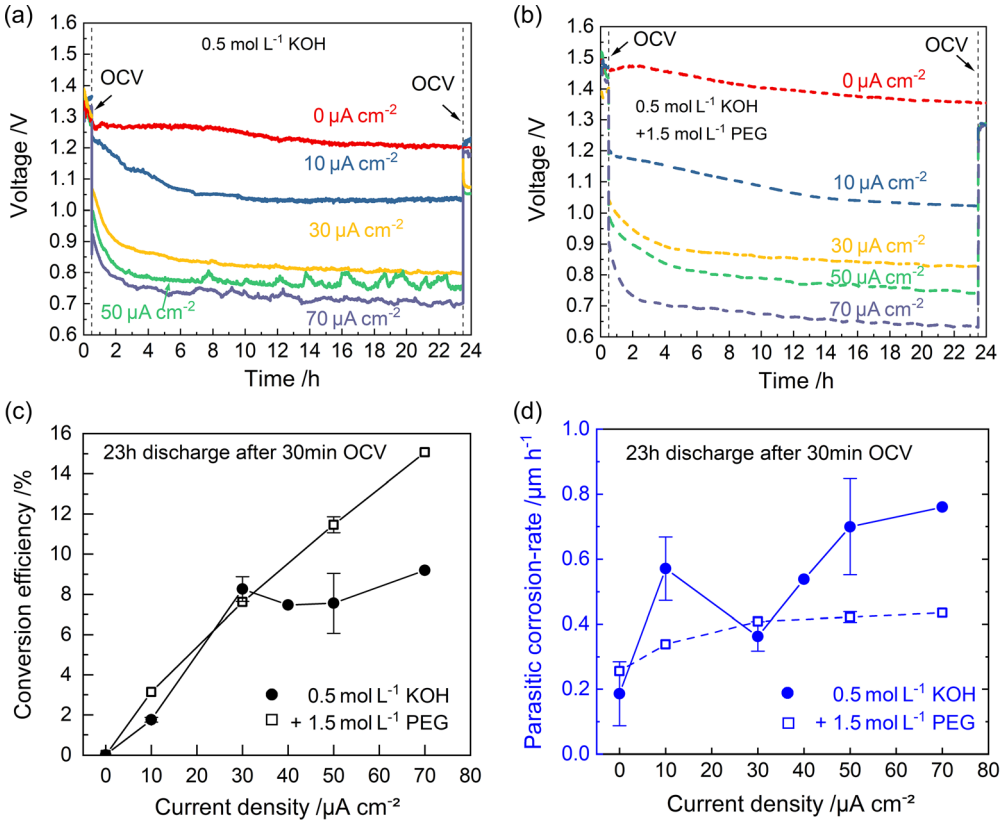

Figure 2. Discharge profiles of SABs at current densities from 0 to 70 µA cm^{-2} in pure 0.5 mol L^{-1} KOH solution a) and with additional 1.5 mol L^{-1} PEG content, b) and their corresponding conversion efficiency c), and parasitic corrosion rate d).

2.2. Electrochemical Performance in Higher pH Electrolyte

The substitution of water with PEG in KOH solutions with low concentration resulted in increased conversion efficiency due to lowered parasitic corrosion (Figure 1 and 2). The discharge duration in 0.5 mol L^{-1} KOH solutions is still limited to below 60 h. Aiming at increasing the discharge duration, we studied the effect of PEG on the performance of SABs with a higher KOH concentration of 2 mol L^{-1}, which is known to result in longer discharge durations, though with lower conversion efficiencies.[9] With increasing PEG amount, the specific energy of the cell rises from 130 Wh kg_{Si}^{-1} in pure 2 mol L^{-1} KOH to 290 Wh kg_{Si}^{-1} with 1 mol L^{-1} PEG 400 (**Figure 3**a). The viscosity increases significantly above 0.1 mol L^{-1} PEG, which results in a reduction of the conductivity from 330 to 70 mS cm^{-1} (Figure 3b). At the same concentration, the average voltage drops from 0.8 to 0.7 V (Figure 3c).

The decrease in voltage with increasing PEG content can be observed in the 24 h discharge profiles (Figure S3, Supporting Information). With a concentration of 0.1 mol L^{-1} PEG, the discharge time prior to passivation of the silicon surface remains above 250 h, similar to that observed in pure 2 mol L^{-1} KOH. However, at a PEG concentration of 1 mol L^{-1} (equivalent to 35% of the volume), the properties of the electrolyte are affected, causing a decrease in conductivity to 72 mS cm^{-1} and a tenfold increase in viscosity. This reduces the discharge time to 150 h (Figure 3c and S4, Supporting Information).

Discharge can occur as long as the reaction products are able to diffuse into the bulk electrolyte. The oxidation peak reduces with increasing PEG (Figure S5, Supporting Information) indicating a reduction of the possible electrochemical reaction rate. Interestingly, the maximum current of 70 µA cm^{-2} that allows a discharge over 24 h stays the same till 1 mol L^{-1} PEG. While a discharge was possible using a 0.5 mol L^{-1} KOH solution and 1.5 mol L^{-1} PEG, it was not viable with 2 mol L^{-1} KOH. Hence, discharge was unsuccessful. At this concentration, 53% of the electrolyte volume consists of PEG, resulting in a reduced water content of 45% (see Table S2, Supporting Information). The higher concentration of OH^- ions present at 2 mol L^{-1} KOH requires more free water molecules for the solvation shell.[39,40] Therefore, fewer free water molecules are available for the solvation shell of the dissociated silicates to diffuse into the bulk electrolyte. Passivation of the silicon surface occurs when this diffusion rate drops below the production rate.[9]

Discharge tests for different durations (Figure 3d) reveal a time-dependent effect on the side reactions. That could be explained by reaction kinetics changing due to the high concentration of silicates in the electrolyte during the later stages of the discharge. The parasitic corrosion rate reduces from 2 µm h^{-1} in

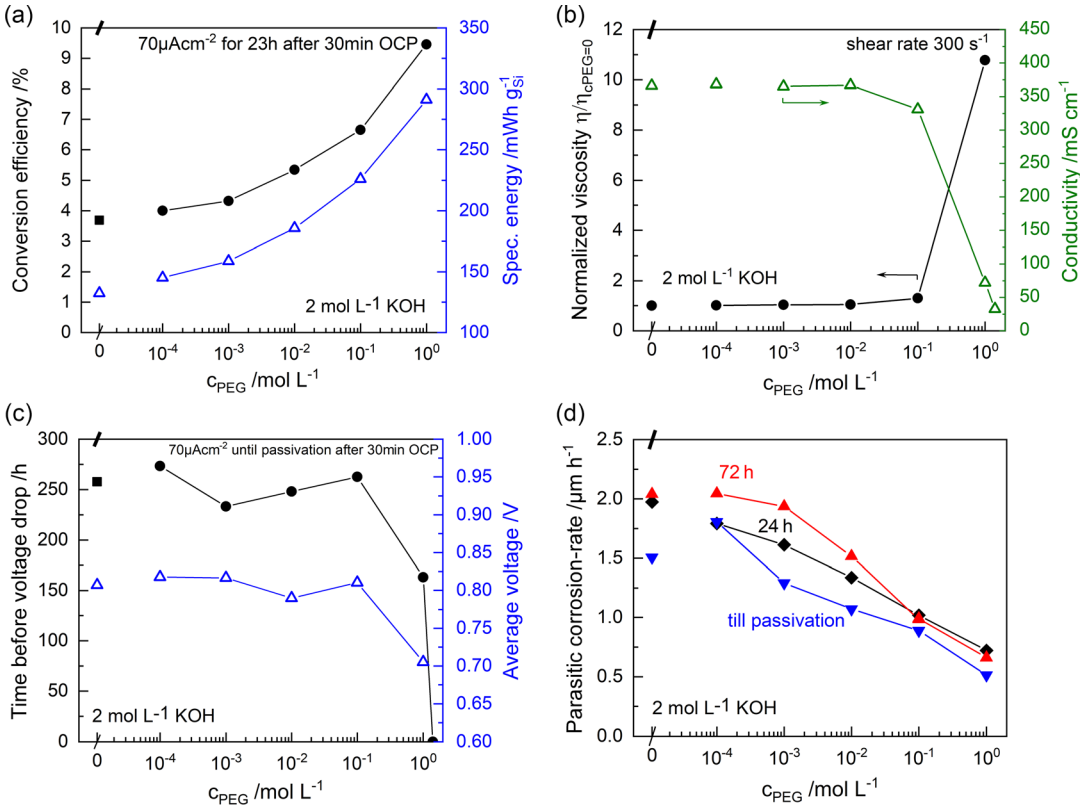

Figure 3. Discharge of SABs in 2 mol L^{-1} KOH solution with varying PEG 400 content: a) The conversion efficiency and specific energy for 23 h after 30 min at OCP, b) the change in viscosity and conductivity due to replacement of water by PEG, c) the time before the passivation of the Si-electrode from discharge tests and their average voltage, d) the change in parasitic corrosion rate for 24, 72 h discharge, and till passivation.

the pure 2 mol L^{-1} KOH solution to 0.7 μm h^{-1} when 1 mol L^{-1} PEG is added. The highly anisotropic etching of silicon in pure KOH leads to the (111) facets of the characteristic pyramidal hillocks on the (100) surface, started by the masking of hydrogen bubble adhesion.[33,36,41,42] An inspection of the silicon surface after 23 h of discharge shows the effect of the PEG-containing KOH electrolyte leaving a mirrorlike finish of the exposed surface area even without magnification. SEM images reveal that the surface is completely covered by pyramids when PEG is absent in agreement with the pitting corrosion under anodic conditions reported in literature.[43] In the presence of PEG, however, few or no pyramids are observed. The higher the PEG concentration, the fewer pyramids are present, until their formation is completely suppressed above 0.01 mol L^{-1} PEG in the 2 mol L^{-1} KOH solution (**Figure 4**). With PEG, the etching turns into a polishing behavior for the (100) plane similar to isopropyl alcohol in KOH.[44] This observation is in contrast to Yang et al. that did not observe significant reduction of surface roughness when etching in a KOH with PEG as an additive under OCP conditions and almost no difference in etch rate.[45] It is important to highlight that we used amounts of PEG that are far larger than the additive concentrations (0.35 mmol L^{-1}) used in their study. At these additive concentrations, we did not observe an improvement in the corrosion behavior of the (100) silicon electrodes either. To confirm a polishing behavior, we prepared silicon nanopyramid structures (Figure S6, Supporting Information), in which silicon nanowire structures turn into upon immersion in KOH.[8] We also prepared porous silicon structures produced by metal assisted electrochemical etching (MAeCE) (Figure S7, Supporting Information). We tested the SABs performance with the textured electrodes in 24 h discharge experiments in in 2 mol L^{-1} KOH with a high PEG content (1 mol L^{-1}) and investigated the resulting surfaces. With PEG in the KOH solution, the structures etched away and the surfaces were left polished after 24 h (Figure S1 and S2, Supporting Information).

Surprisingly, the parasitic corrosion rate of silicon in 2 mol L^{-1} KOH with 1 mol L^{-1} PEG was found to be independent of the various surface structures tested during the 24 h discharge experiments (**Figure 5**). The larger surface area means lower local current densities, which drive the electrochemical reaction. For pure KOH electrolytes, this would result in reduced local parasitic corrosion (as in Figure 2). However, the total corrosion would be expected to increase due to the larger surface area exposed to the electrolyte compared to the flat surface. The increase in parasitic corrosion with the current density was found to be much lower with the high PEG concentration (see Figure 2), leading to a negligible effect of different surface areas. This can also be seen in the voltage profiles during discharge (Figure 5). Further investigations of the underlying mechanisms are needed.

Experiments utilizing PGA diacid (PDA) with a molecular weight of 600 g mol^{-1} exhibited analogous behavior of SABs

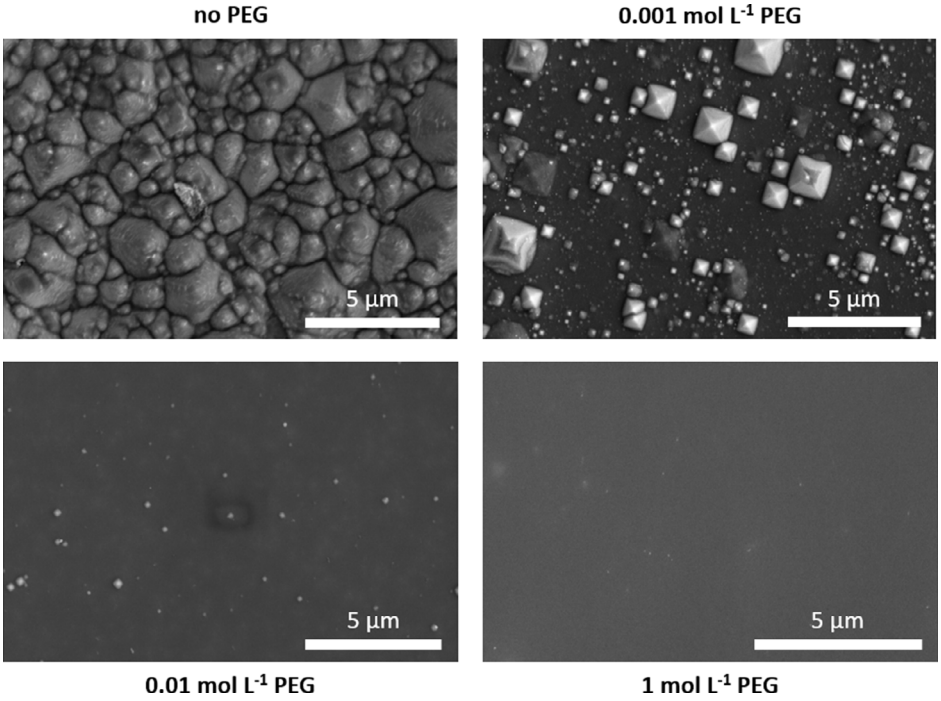

Figure 4. SEM images of silicon electrodes surfaces after the 23 h of discharge (as in Figure 3a) for 2 mol L^{-1} KOH solution without PEG and with increasing PEG content.

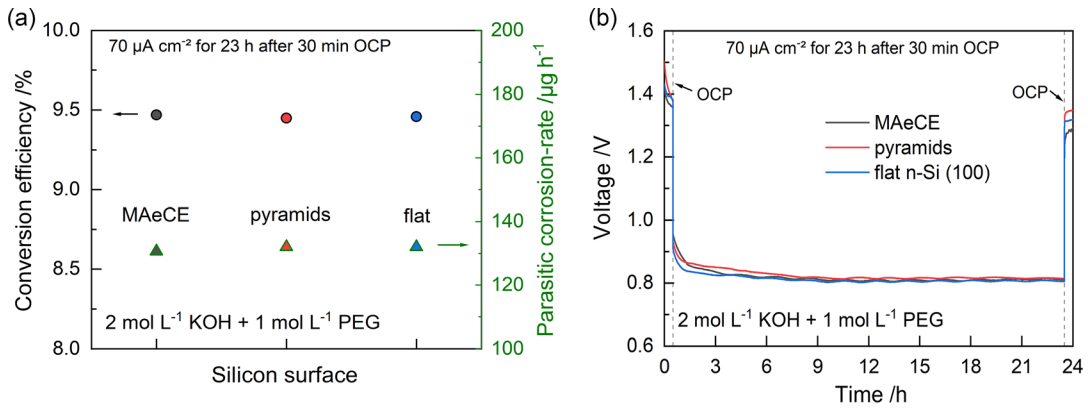

Figure 5. Behavior of different silicon surface structures in SABs with 2 mol L^{-1} KOH and 1 mol L^{-1} PEG after discharge at 70 µA cm^{-2} for 23 h after 30 min OCP with a) conversion efficiency and parasitic corrosion rate and b) the corresponding voltage profiles.

to those employing PEG (**Figure 6**). The effect of carboxyl end groups in PDA and the hydroxyl groups present in PEG seems to have a negligible impact on the discharge characteristics with comparable trends being observed (Figure 6). The highest allowable concentration for PDA was determined to be 0.7 mol L^{-1}, whereas for PEG it was 1 mol L^{-1}. This difference in concentration may potentially be attributed to factors such as pH and molecular weight (Mw). For instance, when considering a 1 mol L^{-1} polymer concentration with 2 mol L^{-1} KOH, PDA represented half of the electrolyte volume, while PEG accounted for only 35%. Therefore, at equivalent concentrations, the volume of water replaced by PDA is significantly greater. Moreover, both electrolytes displayed a limit of 50% replacement of H_2O volume by the polymer beyond which no discharge is possible. Although the voltage also decreases with the addition of PDA (Figure S8, Supporting Information), the specific energy density increases significantly from 140 to 290 Wh Kg_{Si}^{-1}.

We investigated the effect of replacing water with PEG at different concentrations and found a reduction of the corrosion reaction with increasing PEG content as well as an improvement of the conversion efficiency, especially at higher currents while maintaining long discharge times. The etching behavior changes from anisotropic, leaving pyramidal hillocks after etching, to a polishing mechanism resulting in flat surfaces. The underlying mechanism of the reduced corrosion does not result from the hydroxyl end groups of the PEG, as PDA with carboxyl end

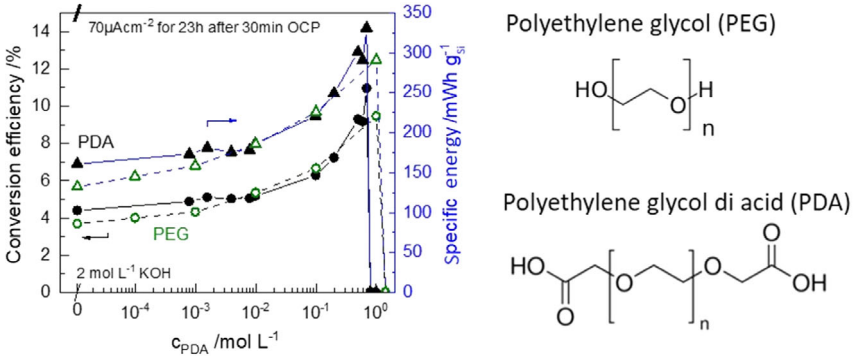

Figure 6. Comparison of the conversion efficiency and specific energy of discharge tests of SABs containing 2 mol L^{-1} KOH with either PEG 400 or PDA 600 and their chemical structures on the right side.

groups shows the same behavior. We attribute this improved performance of the SAB to the reduced availability of water for the parasitic corrosion reaction due to the replacement by the organic molecule. Thus, this system provides a path toward a sustainable battery with nontoxic, widely available materials that can be produced in an environmentally friendly way.

3. Conclusion

SABs with alkaline electrolytes suffer from severe corrosion during discharge. We hypothesized that a reduction of water molecules in the alkaline electrolyte could lead to less parasitic corrosion, as the H_2O attack on the silicon at low KOH concentrations limits the reaction rate. We introduced PEG as a cheap, nontoxic solvent to replace part of the water in the electrolyte solution. We show in discharge tests of full SABs with KOH that PEG can effectively decrease the parasitic corrosion from 2 μm h^{-1} to 0.7 μm h^{-1} by substituting 35% of the water volume in 2 mol L^{-1} KOH solution with PEG. This caused the specific energy to double from 130 to 290 Wh kg_{Si}^{-1}. The same could be observed in 0.5 mol L^{-1} KOH, with an increase of specific energy from 250 Wh kg_{Si}^{-1} in pure KOH up to 384 Wh kg_{Si}^{-1} with 1 mol L^{-1} PEG content. The high PEG concentrations used changed the etching characteristics, from anisotropic with pyramidal hillocks on the silicon surface to a polishing behavior with a flat (100) surface. This could be of interest for silicon micromachining. We found that the performance of the PEG electrolyte is almost independent of the surface area in the investigated range. We also showed that with high amounts of PEG, the parasitic corrosion rate does not increase further at higher currents in contrast to the pure KOH electrolyte. The discharge duration is not negatively affected till 1 mol L^{-1} PEG in 0.5 mol L^{-1} KOH and till 0.1 mol L^{-1} PEG in 2 mol L^{-1} KOH. Tests with PDA revealed that the increase in performance for both polymers is not related to the hydroxyl or carboxyl end groups, but rather the replacement of H_2O molecules. Our results display the potential for SABs improved performance in the presence of PEG, especially at higher discharge currents. Further investigation of the underlying mechanisms, especially the interaction between the PEG chain and the silicates formed during SAB discharge, is needed for further improvement of the performance. Large surfaces should be investigated at higher total currents to determine if the discharge rate can be further increased while corrosion is kept constant.

4. Experimental Section

Chemicals and Materials: The n-type Si (100) wafers (Silicon Materials, 1–10 Ω cm, phosphor doped) with a thickness of 525+/–25 μm were laser cut, cleaned with isopropanol, and then Piranha etching solution (3 parts 98% H_2SO_4 to 1 part 30% H_2O_2) for 10 min and then thoroughly rinsed with deionized water. The native oxide film was removed with 5% HF before assembly in the test cell. Pyramid structures were fabricated according to Sarwar et al.[8] The MAeCE structure was fabricated by metal-assisted electrochemical etching. For this, silver was deposited on n-Si(100) wafer by immersion in 2.5 mol L^{-1} HF with 0.01 mol L^{-1} $AgNO_3$ for 10 s and electrochemical etching in 4 mol L^{-1} HF at 7 V for 20 min with stirring.

Preparation of the Electrolytes: Solutions with KOH concentrations from 0.1 to 5 mol L^{-1} were prepared from KOH pellets (>85%, Sigma Aldrich) and used as the electrolyte. A 2 mol L^{-1} PEG (Mw 400, Alfa Aeser) solution was mixed in 1:1 volume ratio with 4 mol L^{-1} KOH to get a final solution of 2 mol L^{-1} KOH : 1 mol L^{-1} PEG. This mother solution was diluted with 2 mol L^{-1} KOH to yield varying quantities of PEG, while maintaining a constant concentration of KOH. Therefore, the water content was replaced by PEG. Other KOH concentrations were done accordingly. PDA (Mw 600, Alfa Aeser) was used in the same way described for PEG. The solutions' conductivity was measured with a Tetracon 325 (WTW Inolab Cond720) conductometer.

Electrochemical Testing: A commercial air electrode with manganese mixed oxide catalyst on a nickel mesh (Gaskatel, Germany) was used as a reliable and cheap cathode. The test cell is made of/fittings and stainless-steel current collectors and an open hole at the top for electrolyte handling (D = 2.5 mm). The active area of the electrodes in contact with the electrolyte is 10 mm in diameter for all tests. If not noted otherwise, tests were conducted at 25 °C with an electrolyte volume of 1 mL for galvanostatic discharge. Galvanic discharge measurements were performed in 2-electrode configuration with the battery cycler BTS3000 (Neware). The measurements in 3-electrode configuration were performed with the potentiostat/galvanostat VIONIC (Metrohm) in the same cell setup as the 2-electrode configuration. A reversible hydrogen electrode was used as a reference electrode in between the silicon and the air–electrode. The full cells were kept at OCP for 30 min after assembly and then discharged at 70 μA cm^{-2} for different times, followed by 30 min at OCP. The voltage drop below 0.4 V was defined as the criteria for the passivation event. Electrodes were thoroughly rinsed with deionized water and blow dried after disassembly. The weight of the silicon was measured before and after discharge tests using a high precision scale. The specific energy

and reaction rate calculations are based on the weight loss of the silicon anode.

Rheological Testing: Dynamic viscosity measurements were performed at room temperature using an Anton Paar MCR501 Twin-Drive rheometer with stainless steel plates at a shear rate of 300 s^{-1} and normalized with the viscosity of the respective pure KOH solution without PEG.

Supporting Information

Supporting Information is available from the Wiley Online Library or from the author.

Acknowledgements

The authors thank Dr. Juliana Martins de Souza e Silva for the fruitful discussions.

Open Access funding enabled and organized by Projekt DEAL.

Conflict of Interest

The authors declare no conflict of interest.

Data Availability Statement

The data that support the findings of this study are available from the corresponding author upon reasonable request.

Keywords

alkaline, corrosion, polyethylene glycol, silicon–air batteries

Received: July 15, 2023
Revised: August 24, 2023
Published online:

[1] X. Zhang, X. Wang, Z. Xie, Z. Zhou, *Green Energy Environ.* **2016**, *1*, 4.
[2] H. Arai, M. Hayashi, in *Encycl. Electrochem. Power Sources* (Ed: J. Garche), Elsevier, Amsterdam **2009**, pp. 347–355.
[3] J. D. Ocon, G. H. A. Abrenica, J. Lee, *ChemElectroChem* **2016**, *3*, 242.
[4] X. Zhong, H. Zhang, Y. Liu, J. Bai, L. Liao, Y. Huang, X. Duan, *ChemSusChem* **2012**, *5*, 177.
[5] Y. E. Durmus, Ö. Aslanbas, S. Kayser, H. Tempel, F. Hausen, L. G. de Haart, J. Granwehr, Y. Ein-Eli, R.-A. A. Eichel, H. Kungl, *Electrochim. Acta* **2017**, *225*, 215.
[6] A. Epshtein, I. Baskin, M. Suss, Y. Ein-Eli, *Adv. Energy Mater.* **2022**, *12*, 2201626.
[7] A. Inoishi, T. Sakai, Y.-W. Ju, S. Ida, T. Ishihara, *J. Mater. Chem. A* **2013**, *1*, 15212.
[8] S. Sarwar, M. Kim, G. Baek, I. Oh, H. Lee, *Bull. Korean Chem. Soc.* **2016**, *37*, 997.
[9] R. Schalinski, S. L. Schweizer, R. B. Wehrspohn, *ChemSusChem* **2023**, *16*, https://doi.org/10.1002/cssc.202300077.
[10] D. Chen, Y. Li, X. Zhang, S. Hu, Y. Yu, *J. Ind. Eng. Chem.* **2022**, *112*, 271.
[11] D. W. Park, S. Kim, J. D. Ocon, G. H. A. Abrenica, J. K. Lee, J. Lee, *ACS Appl. Mater. Interfaces* **2015**, *7*, 3126.
[12] A. Garamoun, M. B. Schubert, J. H. Werner, *ChemSusChem* **2014**, *7*, 3272.
[13] R. Buckingham, T. Asset, P. Atanassov, *J. Power Sources* **2021**, *498*, 229762.
[14] J. Zhu, Y. Zhou, C. Gao, *J. Power Sources* **1998**, *72*, 231.
[15] T. Wang, H. Cheng, Z. Tian, Z. Li, Z. Lin, Z. You, Y. Lu, Y. Zhu, W. Li, Y. Yang, Q. Zhong, Y. Lai, *Energy Storage Mater.* **2022**, *53*, 371.
[16] S. Malkhandi, B. Yang, A. K. Manohar, G. K. S. Prakash, S. R. Narayanan, *J. Am. Chem. Soc.* **2013**, *135*, 347.
[17] A. Kraytsberg, Y. Ein-Eli, *J. Power Sources* **2011**, *196*, 886.
[18] Y. Ein-Eli, *Electrochem. Solid-State Lett.* **2004**, *7*, 5.
[19] Y. Ein-Eli, M. Auinat, D. Starosvetsky, *J. Power Sources* **2003**, *114*, 330.
[20] Y. Xiao, J. Shi, F. Zhao, Z. Zhang, W. He, *J. Electrochem. Soc.* **2018**, *165*, A47.
[21] M. Liang, H. Zhou, Q. Huang, S. Hu, W. Li, *J. Appl. Electrochem.* **2011**, *41*, 991.
[22] V. K. Nartey, L. Binder, K. Kordesch, *J. Power Sources* **1994**, *52*, 217.
[23] Y. E. Durmus, S. S. Montiel Guerrero, Ö. Aslanbas, H. Tempel, F. Hausen, L. G. J. de Haart, Y. Ein-Eli, R.-A. Eichel, H. Kungl, *Electrochim. Acta* **2018**, *265*, 292.
[24] K. Murata, S. Izuchi, Y. Yoshihisa, *Electrochim. Acta* **2000**, *45*, 1501.
[25] C. C. Yang, S. J. Lin, *J. Power Sources* **2002**, *112*, 497.
[26] C. Fruijtier-Pölloth, *Toxicology* **2005**, *214*, 1.
[27] O. J. Glembocki, E. D. Palik, G. R. de Guel, D. L. Kendall, *J. Electrochem. Soc.* **1991**, *138*, 1055.
[28] E. D. Palik, V. M. Bermudez, O. J. Glembocki, *J. Electrochem. Soc.* **1985**, *132*, 871.
[29] H. G. G. Philipsen, J. J. Kelly, *J. Phys. Chem. B* **2005**, *109*, 17245.
[30] X. H. Xia, J. J. Kelly, *Phys. Chem. Chem. Phys.* **2001**, *3*, 5304.
[31] X. Xia, C. M. A. Ashruf, P. J. French, J. Rappich, J. J. Kelly, *J. Phys. Chem.* **2001**, *105*, 5722.
[32] G. Cohn, D. D. MacDonald, Y. Ein-Eli, *ChemSusChem* **2011**, *4*, 1124.
[33] W. Haiss, P. Raisch, L. Bitsch, R. J. Nichols, X. Xia, J. J. Kelly, D. J. Schiffrin, *J. Electroanal. Chem.* **2006**, *597*, 1.
[34] O. J. Glembocki, R. E. Stahlbush, M. Tomkiewicz, *J. Electrochem. Soc.* **1985**, *132*, 145.
[35] H. Weinrich, Y. E. Durmus, H. Tempel, H. Kungl, R. A. Eichel, *Materials* **2019**, *12*, 21341.
[36] H. Seidel, L. Csepregi, A. Heusberger, H. Baumgärtel, A. Heuberger, H. Baumgärtel, *J. Electrochem. Soc.* **1990**, *137*, 3626.
[37] H. G. G. Philipsen, F. Ozanam, P. Allongue, J. J. Kelly, J.-N. Chazalviel, *J. Electrochem. Soc.* **2016**, *163*, H327.
[38] G. Cohn, D. Starosvetsky, R. Hagiwara, D. D. Macdonald, Y. Ein-Eli, *Electrochem. Commun.* **2009**, *11*, 1916.
[39] Z. Zhu, M. E. Tuckerman, *J. Phys. Chem. B* **2002**, *106*, 8009.
[40] B. Chen, I. Ivanov, J. M. Park, M. Parrinello, M. L. Klein, *J. Phys. Chem. B* **2002**, *106*, 12006.
[41] J. W. Faust, E. D. Palik, *J. Electrochem. Soc.* **1983**, *130*, 1413.
[42] P. Raisch, W. Haiss, R. Nichols, D. Schiffrin, *Electrochim. Acta* **2000**, *45*, 4635.
[43] P. Allongue, V. Costa-Kieling, H. Gerischer, *J. Electrochem. Soc.* **1993**, *140*, 1018.
[44] K. P. Rola, I. Zubel, *Microsyst. Technol.* **2013**, *19*, 635.
[45] C. R. Yang, P. Y. Chen, C. H. Yang, Y. C. Chiou, R. T. Lee, *Sens. Actuators, A Phys.* **2005**, *119*, 271.